Published in final edited form as:
Chem Mater. 2012 November 13; 24(21): 4036–4042. doi:10.1021/cm3011524.

Mesostructured Block Copolymer Nanoparticles: Versatile Templates for Hybrid Inorganic/Organic Nanostructures

Luke A. Connal[1], **Nathaniel A. Lynd**[1], **Maxwell J. Robb**[2], **Kimberly A. See**[1], **Se Gyu Jang**[1], **Jason M. Spruell**[1], and **Craig J. Hawker**[1,2]

[1]Materials Research Laboratory and Materials Department, University of California, Santa Barbara, California 93106

[2]Department of Chemistry and Biochemistry, University of California, Santa Barbara, California 93106

Abstract

We present a versatile strategy to prepare a range of nanostructured poly(styrene)-*block*-poly(2-vinyl pyridine) copolymer particles with tunable interior morphology and controlled size by a simple solvent exchange procedure. A key feature of this strategy is the use of functional block copolymers incorporating reactive pyridyl moieties which allow the absorption of metal salts and other inorganic precursors to be directed. Upon reduction of the metal salts, well-defined hybrid metal nanoparticle arrays could be prepared, while the use of oxide precursors followed by calcination permits the synthesis of silica and titania particles. In both cases, ordered morphologies templated by the original block copolymer domains were obtained.

Keywords

Block copolymer; nanoparticle; self-assembly; templating; morphology

Introduction

The dramatic increase in surface area associated with polymeric nanoparticles has sparked interest in applications ranging from biomedicine to photovoltaics.[1–12] However, most of this interest and related design strategies have focused on the surface properties of these nanostructures,[13–14] with only a limited number of studies examining strategies to control and exploit internal morphology. This is unfortunate since controlled internal structure creates significant opportunities for further increasing surface area while also providing unique nanoenvironments for the spatial location of functional groups within these systems, template porous silica particles being an excellent example.[15]

In terms of nanoscale morphologies, block copolymers (BCP) offer a wide variety of self-assembled structures in solution,[16–17] for example micelles,[18] vesicles,[19] and rods[20–21] while the same block copolymers undergo phase separation induced self-assembly in the bulk or in thin films, to give various nanoscale morphologies including lamellae, hexagonally-packed cylinders, spherical and gyroid structures.[22] To combine the shape and size control of solution assembly with the richness of bulk morphologies, two strategies

Correspondence to: Craig J. Hawker.

Supporting Information Available

Methods, synthetic procedures, and complete characterization of materials. This information is available free of charge via the Internet at http://pubs.acs.org.

have recently been developed to allow the self-assembly of BCPs into nanoparticles with subsequent internal phase-separation leading to a range of ordered nanostructures. [23–25] The first technique emulsifies a BCP with appropriate surfactants and water-immiscible solvents and the phase-separated nanostructure is then formed after the organic solvent is removed.[24] The second strategy involves a solvent exchange procedure using a water-miscible solvent and has the advantage of not requiring surfactants. In this case the polymer is dissolved in a good solvent and a bad solvent is gradually added to induce particle formation[25] with the internal nanostructures being controlled by block copolymer phase separation. While this technique affords access to novel nanostructures,[26] with applicability in drug delivery[27] there has been limited success in controlling the size of these nanoparticles, or in exploiting the internal functional groups.

The preparation of mesostructured oxide particles is a well developed field utilizing the self assembly of small organic surfactants or even amphiphilic polymer block copolymers.[28] However, the utilization of hydrophobic block copolymers to guide the sol-gel reactions enables access to new libraries of self assembled structures. The morphology and size of the features can be tuned by the block copolymer volume fraction and molecular weights of the block copolymer, thus enabling the preparation of silica layers in size ranges that are unachievable by current methods.[29] Likewise the preparation of layered structures with metal nanoparticles has been developed utilizing layer-by-layer,[30] however these stepwise procedures do not allow the versatility of controlling internal phase separated morphologies. Herein, we present a versatile strategy to prepare a range of nanostructured particles with tunable interior morphology and controlled size by a simple solvent exchange procedure. By selecting poly(styrene)-*b*-poly(2-vinyl pyridine) (PS-*b*-P2VP) as the block copolymer, a unique library of structures with variable internal morphology through thermal or solvent-annealing can be obtained. In addition, the pyridine unit can be exploited as a functional handle to form hybrid metal nanoparticle loaded polymer particles and to template the condensation of silica or titania to produce nanostructured oxide particles. These generalized strategies allow a range of structures to be prepared (Scheme 1) and may find use in diverse applications from catalysis and surface enhanced Raman spectroscopy to photovoltaic devices.[31–33]

Results and Discussion

Due to its well-known phase behavior,[34] PS-*b*-P2VP was initially chosen to investigate the interplay between nanoparticle formation and internal morphology. Two different polymers based on PS-*b*-P2VP were utilized, one a diblock copolymer PS-*b*-P2VP (M_n = 19 KDa, f_{P2VP}= 25%) and the other a triblock copolymer PS-*b*-P2VP-*b*-PS (M_n = 16 KDa, f_{P2VP} = 38%). The preparation of polymer nanoparticles by a slow evaporation strategy involves the initial dissolution of the BCP in tetrahydrofuran (THF, 0.1 wt%) with water being added at the rate of 1 mL/min to the polymer solution with constant stirring until the final water to THF ratio of 2:1 is obtained. THF is then allowed to slowly evaporate under ambient conditions over the course of three days. Utilizing this procedure, both the PS-*b*-P2VP diblock and the PS-*b*-P2VP-*b*-PS triblock copolymers formed nanoparticles, with the P2VP phase-separating into ordered P2VP spheres with 10.5 ±1.2 nm diameters (measured from TEM images) within a PS matrix (Figure 1).

Interestingly, the diblock copolymer formed dimple, or bowl-like particles (Figures 1a and 1b). These bowl-like structures have been observed in other colloidal systems[35] with the unique shape possibly originating from the initial formation of a glassy skin around the particle. Upon further change in solvent conditions, the THF escapes by rupturing the surface of the particle to form a dimple/hole. While the PS-*b*-P2VP-*b*-PS triblock copolymer forms spherical nanoparticles without any dimples, phase separation to give a spherical

internal morphology is again observed (Figures 1c and 1d). These systems show remarkable ordering of the internal 10 nm features without annealing, which is dramatically different to the corresponding bulk systems. In fact, these same di- and triblock copolymers have vastly different morphologies in the bulk, with both exhibiting ill-defined morphologies with very poor order, even after extended annealing (Figure S1), possibly due to the relatively low molecular weight of the copolymers used. This illustrates the dramatic influence that nanoconfinement can play in the preparation of ordered nanoscale morphologies.[36]

The success of this initial demonstration of controlled phase morphologies in block copolymer nanoparticles prompted an investigation into controlling particle size. Under these initial conditions, dynamic light scattering (DLS) measurements indicated that the PS-*b*-P2VP diblock copolymer formed particles with a diameter of around 400 nm and the PS-*b*-P2VP-*b*-PS triblock copolymer formed particles with diameter of 600nm. To further understand size control and the *in situ* evolution of particle size for these systems, a comprehensive light scattering study was performed whereby particle growth was monitored during water addition (Figure 2). Upon addition of water, aggregates are immediately observed for both systems with the diameter of the particles formed from the diblock copolymer increasing with increasing water concentration, reaching a plateau of approximately 400nm at a 30 wt% water concentration (THF:H20; 30:70). A similar sensitivity is demonstrated by the PS-*b*-P2VP-*b*-PS triblock where water addition leads to a similar plateau after addition of 40wt% water. It is postulated that the onset of the plateau in both cases occurs when the solvent-environment is too hydrophilic to allow BCP exchange between particles. Importantly, these results demonstrate that particle size can be controlled by regulating the amount of water added during particle formation. The biggest challenge in exploiting this strategy to control particle sizes is “quenching”, or stopping, of particle growth. By rapid injection of excess water into the solvent/polymer mixture, further growth of the particles was stopped while at the same time effectively locking the particle size to that determined by the amount of water initially added during the slow addition phase. As illustrated in figure 3, a distinct relationship between the amount of water added and particle size was possible with particles prepared from the triblock copolymer reproducibly leading to particles with diameters of 75, 240, and 560 nm after addition of 7.5 %wt, 14 %wt, and 28 %wt water, respectively. Similar results were obtained for the diblock copolymer, clearly demonstrating that this is a robust strategy for the preparation of particles with controlled diameters in the range of 50–500 nm.

Once formed, these particles are stable in aqueous to size changes due to the insolubility of the diblock and triblock copolymer chains. An advantage of this insolubility and associated static particle size is that these systems can be annealed to control the internal morphology as well as obtain thermodynamically stable nanostructures. Both thermal and solvent-assisted techniques were adapted from traditional thin film procedures with thermal annealing involving the heating of a stable dispersion of nanoparticles in water at 80 °C. Significantly, thermal annealing resulted in a dramatic change in morphology for these block copolymer particles which is illustrated for the triblock copolymer where the transition from P2VP spheres in a PS matrix to a well-ordered, lamella-like or layered morphology is observed (Figures 4a and 4b). Similar structural changes were observed for the triblock copolymer under modified solvent-annealing conditions. In this case the particles are formed as before, however the system is sealed before the THF has completely evaporated but after stable particles have been formed. Upon sealing this system the particles were left to stand at 40 °C for 48 h. Of particular note is the difference in behavior between the triblock and diblock copolymers. No change in morphology was observed for the diblock copolymer particles under either thermal- or solvent-annealing conditions, likewise the dimple structure did not change upon annealing. This may be due to the higher P2VP composition and the different polymeric architectures. The nature of the internal morphology was also found to

be dependent on the size of the particle. As can be seen in Figure 4a and 4b, large 400 nm particles formed from the triblock copolymer underwent a well-behaved transition from spherical morphology to layered/lamella morphology on annealing. In direct contrast, smaller 250 nm particles formed from the same triblock copolymer and annealed under identical thermal conditions formed a disordered lamella phase (Figure 4d). This behavior may be due to confinement or commensurability with the highly-curved interior wall of the particle at small particle diameters.[37]

One of the challenges in nanoparticle research is the controlled introduction of functional units within the interior of the nanostructure, there has been some recent examples of elegant procedures to prepare inorganic/organic hybrids.[38] Here we have developed a versatile technique based on The incorporation of the pyridine moiety which allows for systematic and generalizable use of this group as a coordinating ligand for various applications.[39] To demonstrate this feature, a range of metal ions could be coordinated inside the polymer particles, including Au, Pd, and Pt, via specific interactions with the P2VP repeat units. Subsequent reduction ultimately afforded the metal nanoparticle-loaded polymer particles with the fidelity of this templation being examined using a variety of techniques. As an example, BCP particles were imaged prior to introduction of metal salt (and without iodine staining) as a control experiment and revealed no contrast variation via TEM (Figure 5a). Upon incubation with Gold chloride trihydrate, the TEM image clearly indicates phase contrast with the dark P2VP domains indicating absorption of the gold salt in the P2VP phase (Figure 5b). The PVP phase has will be starting to swell and thus will enable the particles to incorporate the metal ions throughout the particle as indicated by the contrast in the TEM images, some layers of the assembly have started to merge allowing further incorporation of metal ions. These particles can be subsequently treated with sodium borohydride to reduce the gold salt and form sub 10 nm gold nanoparticles imbedded into the parent polymer particles (Figure 5c). The incorporation of gold into the nanoparticles was also confirmed by Energy-dispersive X-ray spectroscopy which showed characteristic Au_L and Au_M lines (Figure S3). Similar results were observed with other metal systems such as Pt and Pd (Figure S4 and S5), which demonstrates the versatility of this approach to hierarchically ordered composite nanoparticles which may be useful in catalysis and surface-enhanced Raman spectroscopy.

The pyridine functionality can be further exploited as a structure directing agent for the production of unique mesostructured silica and titania particles. Simply mixing the preformed nanostructured polymer particles with a hydrolyzed aqueous silica or titania solution successfully directed the template condensation of the oxide precursors. To illustrate this strategy the triblock copolymer particles shown in Figure 4a were used as templates and after formation of the hybrid silica-polymer particle (Figure S6), the BCP template could be removed by calcination at 400 °C for 2 h, which was verified by TGA (Figure S7). The resultant oxide particles revealed a mesoporous structure with high fidelity of the original phase separated polymer domains (Figure 6a), nitrogen isotherm confirmed mesoporous structure (Figure S8). The same procedure could be repeated with a titania precursor (Figure S9), furthermore, the initial lamellae triblock copolymer particle can be utilized (Figure 4b) which allowed the formation of ‘onion-like’ TiO_2 nanoparticles with complete removal of the organic template (Figure 6b), similarly a layered silca particle can also be synthesized (Figure S10).

Conclusions

By exploiting the combination of microscale solution assembly of block copolymers with the solid-state phase separation of block copolymer domains, a robust procedure for controlling the size and the interior morphology of BCP nanoparticles has been developed.

Polymer particles with interior morphology were readily prepared, gaining access to a rich array of nanostructures from 50 to 500 nm in diameter. The versatility of this strategy also allows functional handles, such as pyridyl groups, to be incorporated into the block copolymer, creating a unique platform for the controlled localization of reactive groups into specific nanoenvironments. Utilizing directed templation, the initial self-assembled nanoscale morphology of the particle can be translated into the corresponding inorganic/organic hybrids or pure inorganic nanostructures with a high degree of fidelity, providing new strategies for complex mesostructured oxide particles.

Experimental

Materials

All reagents were purchased from Sigma Aldrich unless otherwise specified. Gold chloride trihydrate ($HAuCl_4.3H_20$, 99.9%), palladium chloride ($PdCl_2$, 99%) chloroplatinic acid ($H_2PtCl_6.6H_20$, ACS reagent) where used as received. Dry THF was used directly from a solvent purification system.[40] Styrene was stirred over CaH_2 and degassed through three freeze-pump-thaw cycles, followed by distillation from dibutyl-magnesium to a flame-dried buret immediately prior to use. 2-vinyl-pyridine was stirred and degassed over triethylaluminum, and distilled to a flame-dried buret immediately prior to use. Water was purified using a millipore water purification system.

Polymer synthesis

Burets containing dry THF, purified styrene, and purified 2-vinyl-pyridine were attached to a flame-dried reactor under an argon atmosphere. The reactor assembly was again flame-dried and cycled between vacuum (5 mTorr) and a positive-pressure argon atmosphere five times. Under an argon atmosphere, THF was added and the reactor temperature was decreased to −70 °C. Styrene was added to the reactor followed by a predetermined amount of sec-butyllithium initiator (1.4M in hexane). Polymerization of styrene was allowed to proceed for 1.5h, 2-vinylpyridine was then added and polymerization continued for an additional 1.5h. The polymerization was terminated with degassed isopropanol. The PS-*b*-P2VP was precipitated in hexanes, filtered, and dried in vacuo. ^{1}H NMR spectroscopy: Mn = 19 kDa, X_{P2VP} = 25%. Size-exclusion chromatography relative to PS-standards: PDI = 1.13. For the PS-*b*-P2VP-*b*-PS triblock polymer: the same procedure as above was performed except termination was performed with a half molar equivalent of *p*-xylene dibromide in THF to couple the living poly(2-vinyl-pyridinyl) chains. ^{1}H NMR spectroscopy: Mn = 16 kDa, X_{P2VP} = 38%. Size-Exclusion Chromatography relative to PS-standards: PDI = 1.18.

Self-assembly of BCP into nanoparticles

The block copolymer was dissolved in THF (4.5 mL, 0.1 wt %) and the solution was continuously stirred while water was added (9mL @ 1 mL/min). The solution was then allowed to stand under ambient conditions to evaporate THF (typically 3 days). For quenched systems, excess water was rapidly injected after the initial slow addition of water followed by THF evaporation. All assembly was conducted at 20°C in 20 mL vials with an open top of 12 mm diameter. Thermal annealing of particles was performed in a water dispersion (0.05 wt%) heated to 80 °C for 48 h. Quasi-solvent annealing was performed by sealing the particle/THF/water mixture before all THF was evaporated (after 48h) and heating to 40 °C for 48 h.

Preparation of metal loaded nanoparticles

To an aqueous dispersion of block copolymer particles (1mL, 0.05 wt%) a solution of metal precursor (100 μL, 0.1 mmol) was added and stirred for 3h. Excess metal was removed by

three centrifugation/dispersion cycles. The metal coordinated in the particles was reduced by addition of $NaBH_4$ solution (100 μL, 0.1 mmol) with stirring for 1h. The particles were purified by three centrifugation/dispersion cycles.

Preparation of oxide nanoparticles

Methods were adapted from previously reported procedures block copolymer thin films[41] using prehydrolyzed solution of oxide precursors. For a silica sol: tetrethyl orthosilicate (TEOS, 0.5 g) was mixed with HCl (0.75 g, 0.2 M), water (0.45 g), and ethanol (1.13 g) and the solution was heated to 60°C for 1h. For the corresponding titania sol: titanium isopropoxide (0.4 g) was mixed with HCl (0.3 g, 12.1 M) and was stirred vigorously for 5 min after which ethanol (1 mL) was added. An aliquot (100 μL) of the hydrolyzed solution was then added to a dispersion of block copolymer particles (3 mL, 0.05 wt %) and stirred for 0.5h. The particles were purified by repeated centrifugation and dispersion cycles and dispersed in water. The water was removed by lyophilization and the particles were subsequently heated to 400 °C in air for 2h to remove the block copolymer template.

Characterization

Transmission electron microscopy was conducted on a FEI-T20 instrument, operating at 200 kV. Grids were prepared by casting a concentrated dispersion of particles onto the copper grids and the droplet was wicked through the grid using tissue paper. Particle dispersions were cast onto freshly cleaned silicon wafers, coated with a gold layer and visualized using Scanning electron microscopy (SEM) on a FEI XL30 Sirion FEG microscope.

Dynamic light scattering measurements were performed on a Wyatt DynaPro NanoStar instrument using Dynamics 7.0 software. Data were collected at 25 °C with an acquisition time of 5 sec. Hydrodynamic radii were averaged over 20 acquisitions. Solvent refractive index values were calculated based on volume composition from independent measurements on aqueous THF solutions performed on a Wyatt Optilab rEX instrument. Viscosities of the binary solvent mixtures were calculated from previously reported data.[42]

Supplementary Material

Refer to Web version on PubMed Central for supplementary material.

Acknowledgments

Funding from an Australian Research Council International Fellowship (LAC), Australian American Association Sir Keith Murdoch Fellowship (LAC), and DOE Office of Science for a graduate fellowship (DOE SCGF) (MJR) is gratefully acknowledged. This work was also supported by the MRSEC Program of the National Science Foundation under Award DMR-1121053 (CJH, MJR, LAC, KAS) and in part with Federal funds from the National Heart, Lung, and Blood Institute, National Institutes of Health, Department of Health and Human Services, as a Program of Excellence in Nanotechnology Contract No. HHSN268201000046C (NAL, JMS, CJH).

References

1. a) Kawaguchi H. Prog. Polym. Sci. 2000; 25:1171–1210.b) Dendukuri D, Doyle PS. Adv. Mater. 2009; 21:4071–4086.
2. a) Matijevic E. Langmuir. 1994; 10:8–16.b) Freeman RG, Grabar KC, Allison KJ, Bright RM, Davis JA, Guthrie AP, Hommer MB, Jackson MA, Smith PC, Walter DG, Natan MJ. Science. 1995; 267:1629–1632. [PubMed: 17808180]
3. a) Pacholski C, Kornowski A, Weller H. Angew. Chem. Int. Ed. 2002; 41:1188–1191.b) Srivastava S, Santos A, Critchley K, Kim K-S, Podsiadlo P, Sun K, Lee J, Xu C, Lilly GD, Glotzer SC, Kotov NA. Science. 2010; 327:1355–1359. [PubMed: 20150443] c) Klajn R, Bishop KJM, Fialkowski M,

Paszewski M, Campbell CJ, Gray TP, Grzybowski BA. Science. 2007; 327:261–264. [PubMed: 17431176]

4. Chandler D. Nature. 2005; 437:640–647. [PubMed: 16193038]
5. Nohynek GJ, Lademann J, Ribaud C, Roberts MS. Critical Reviews in Toxicology. 2007; 37:251–277. [PubMed: 17453934]
6. a) Zelikin AN. ACS Nano. 2010; 4:2494–2509. [PubMed: 20423067] b) Soike T, Streff AK, Guan C, Ortega R, Tantawy M, Pino C, Shastri VP. Adv. Mater. 2010; 22:1392–1397. [PubMed: 20437489] c) Ochs CJ, Such GK, Yan Y, van Koeverden MP, Caruso F. ACS Nano. 2010; 4:1653–1663. [PubMed: 20201548]
7. a) Thomas JM, Johnson BFG, Raja R, Sankar G, Midgley PA. Acc. Chem. Res. 2003; 36:20–30. [PubMed: 12534301] b) Mazumder V, Lee Y, Sun S. Adv. Funct. Mater. 2010; 20:1224–1231.
8. Fan JA, Wu C, Bao K, Bao J, Bardhan R, Halas NJ, Manoharan VN, Nordlander P, Shvets G, Capasso F. Science. 2010; 328:1135–1138. [PubMed: 20508125]
9. a) Shokeen M, Pressly ED, Hagooly A, Zheleznyak A, Ramos N, Fiamengo AL, Welch MJ, Hawker CJ, Anderson CJ. ACS Nano. 2011; 5:738–747. [PubMed: 21275414] b) Pressly ED, Rossin R, Hagooly A, Fukukawa K-I, Messmore BW, Welch MJ, Wooley KL, Lamm MS, Hule RA, Pochan DJ, Hawker CJ. Biomacromolecules. 2007; 8:3126–3134. [PubMed: 17880180]
10. Keng P, Bull MM, Shim I-B, Armstrong NR, Pyun J. Chem. Mater. 2011; 23:1120–1129.
11. Peng H, Blakey I, Dargaville B, Rasoul F, Rose S, Whittaker AK. Biomacromolecules. 2009; 10:374–381. [PubMed: 19128056]
12. Du J, O'Reilly RK. Chem. Soc. Rev. 2011; 40:2402–2416. [PubMed: 21384028]
13. Caruso F. Adv. Mater. 2001; 13:11–22.
14. a) Goh TK, Guntari SN, Ochs CJ, Blencowe A, Mertz D, Connal LA, Such GK, Qiao GG, Caruso F. Small. 2011; 20:2863–2867. [PubMed: 21990191] b) Mertz D, Ochs CJ, Zhu ZY, Lee L, Guntari SN, Such GK, Goh TK, Connal LA, Blencowe A, Qiao GG, Caruso F. Chem. Comm. 2011; 47:12601–12603. [PubMed: 22045048]
15. Zhao Y, Jiang L. Adv. Mater. 2009; 21:3621–3638.
16. For reviews see Riess G. Prog. Polym. Sci. 2003; 28:1107–1170. Gohy J-F. Adv. Polym. Sci. 2005; 190:65–136. Hayward RC, Pochan DJ. Macromolecules. 2010; 43:3577–3584.
17. Pochan D, Zhu J, Zhang K, Wooley KL, Miesch C, Emrick T. Soft Matter. 2010; 7:2500–2506.
18. Schacher F, Walther A, Müller AHE. Langmuir. 2009; 25:10962–10969. [PubMed: 19537738]
19. Cottenye N, Syga M-I, Nosov S, Müller AHE, Ploux L, Vebert-Nardin C. Chem. Commun. 2012; 48:2615–2617.
20. a) Lee E, Hammer B, Kim JK, Page Z, Emrick T, Hayward RC. J. Am. Chem Soc. 2011; 133:10390–10393. [PubMed: 21627317] b) Bokel FA, Sudeep PK, Pentzer E, Emrick T, Hayward RC. Macromolecules. 2011; 44:1768–1770.
21. Petzetakis N, Dove AP, O'Reilly RK. Chem. Sci. 2011; 2:955–960.
22. a) Bates FS, Fredrickson GH. Annu. Rev Phys. Chem. 1990; 41:525–557. [PubMed: 20462355] b) Ruzette AV, Leibler L. Nat. Mater. 2005; 4:19–31. [PubMed: 15689991] c) Bang J, Jeong U, Ryu DY, Russell TP, Hawker CJ. Adv. Mater. 2009; 21:4769–4792. [PubMed: 21049495] d) Xu T, Stevens J, Villa JA, Goldbach JT, Guarim KW, Black CT, Hawker CJ, Russell TR. Adv. Funct. Mater. 2003; 13:698–702.e) Jeong UY, Kim HC, Rodriguez RL, Tsai IY, Stafford CM, Kim JK, Hawker CJ, Russell TP. Adv. Mater. 2002; 14:274.
23. a) Lu Z, Liu G, Liu F. Macromolecules. 2001; 34:8814–8817.b) Okubo M, Saito N, Takeoh R, Kobayashi H. Polymer. 2005; 46:1151–1156.c) Jeon S-J, Yi G-R, Koo CM, Yang S-M. Macromolecules. 2007; 40:8430–8439.d) Jeon S-J, Yang S-M, Kim BJ, Petrie JD, Jang SG, Kramer EJ, Pine DJ, Yi G-R. Chem. Mater. 2009; 21:3739–3741.
24. Jeon S-J, Yi G-R, Yang S-M. Adv. Mater. 2008; 20:4103–4108.
25. a) Yabu H, Higuchi T, Ijiro K, Shimomura M. Chaos. 2005; 15:047505/1–047505/7. [PubMed: 16396598] b) Yabu H, Higuchi T, Shimomura M. Adv. Mater. 2005; 17:2062–2065.c) Higuchi T, Tajima A, Yabu H, Shimomura M. Soft Matte. 2008; 4:1302–1305.d) Higuchi T, Tajima A, Motoyoshi K, Yabu H, Shimomura M. Angew. Chem. Int. Ed. 2008; 47:8044–8046.

26. Higuchi T, Tajima A, Motoyoshi K, Yabu H, Shimomura M. Angew. Chem. Int. Ed. 2009; 48:5125.
27. Robb MJ, Connal LA, Lee BF, Lynd NA, Hawker CJ. Polym. Chem. 2012; 3:1618–1628.
28. Berggren A, Palmqvist AEC, Holmberg K. Soft Matter. 2005; 1:219–226.
29. a) Dongyuan Z, Yang P, Huo Q, Chmelka BF, Stucky GD. Current Opinion in Solid State and Materials Science. 1998; 3:111–121.b) Ren Y, Ma Z, Bruce PG. Chem. Soc. Rev. 2012; 41:4909–4927. .3. [PubMed: 22653082] b) Wan Y, Zhao D. Chem. Rev. 2007; 107:2822.
30. Caruso F, Spasova M, Susha A, Giersig M, Caruso RA. Chem. Mater. 2001; 13:109–116.
31. Fan Q-H, Li YM, Chan ASC. Chem. Rev. 2002; 102:3385–3466. [PubMed: 12371889]
32. Alvarez-Puebla RA, Liz-Marzán LM. Chem. Soc. Rev. 2012; 41:43–51. [PubMed: 21818469]
33. Jose R, Thavasi V, Ramakrishna S. J. Am. Ceram. Soc. 2009; 92:289–301.
34. Schulz MF, Khandpur AK, Bates FS, Almdal K, Mortensen K, Hajduk DA, Gruner SM. Macromolecules. 1996; 29:2857–2867.
35. a) Liu X, Kim J-S, Wu J, Eisenberg A. Macromolecules. 2005; 38:6749–6751.b) Riegel IC, Eisenberg A. Langmuir. 2002; 18:3358–3363.c) Saito N, Kagari Y, Okubo M. Langmuir. 2006; 22:9397–9402. [PubMed: 17042560]
36. Huck WTS. Chem. Commun. 2005:4143–4148.
37. Wu Y, Cheng G, Katsov K, Sides SW, Wang J, Tang J, Fredrickson GH, Moskovits M, Stucky GD. Nat. Mater. 2004; 3:816–822. [PubMed: 15502836]
38. a) Lim J, Yang H, Paek K, Cho C-H, Kim S, Bang J, Kim BJ. J. Polym. Sci. Part A: Polym. Chem. 2011; 49:3464–3474.b) van Berkel KY, Hawker CJ. J. Polym. Sci. Part A: Polym. Chem. 2010; 48:1594–1606.c) Yamada S, Mouri E, Yoshinaga K. J. Polym. Sci. Part A: Polym. Chem. 2011; 49:712–718.
39. Bronstein LM, Sidorov SN, Valetsky PM. Langmuir. 1999; 15:6256–6262.
40. Pangborn AB, Giardello A, Grubbs RH, Rosen RK, Timmers FJ. Organomet. 1996; 15:1518.
41. a) Hayward RC, Chmelka BF, Kramer EJ. Adv. Mater. 2005; 17:2591–2595.b) Hayward RC, Chmelka BF, Kramer EJ. Macromolecules. 2005; 38:7768–7783.c) Chen D, Park S, Chen J-T, Redston E, Russell TP. ACS Nano. 2009; 3:2827–2833. [PubMed: 19719151]
42. Aminabhavi TM, Gopalakrishna B. J. Chem. Eng. Data. 1995; 40:856–861.

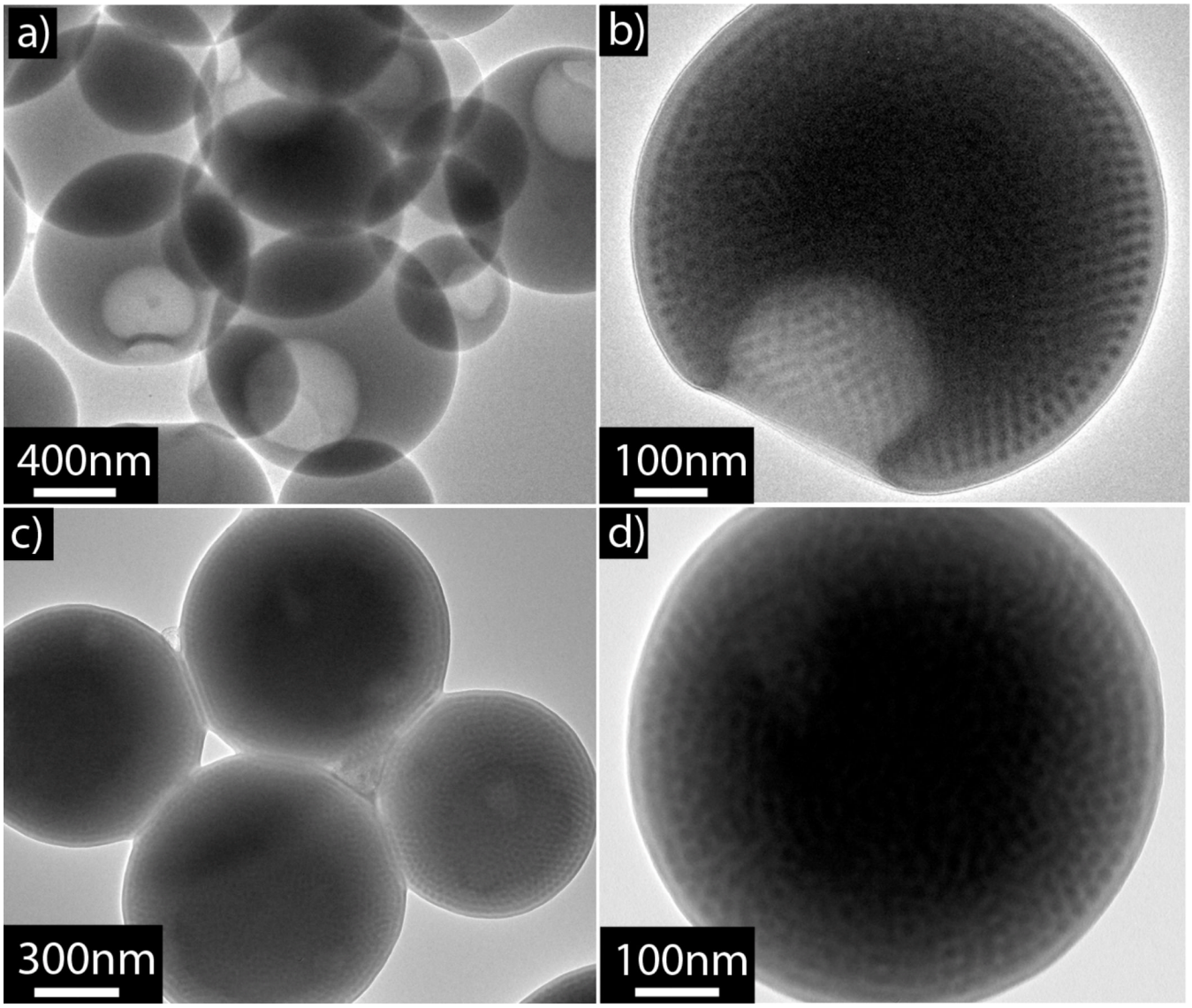

Figure 1.
(a) and (b) TEM of phase-separated particles formed by PS-*b*-P2VP diblock copolymers. (c) and (d) TEM of phase-separated, spherical particles formed by PS-*b*-P2VP-*b*-PS triblock copolymers. P2VP phase is stained with iodine.

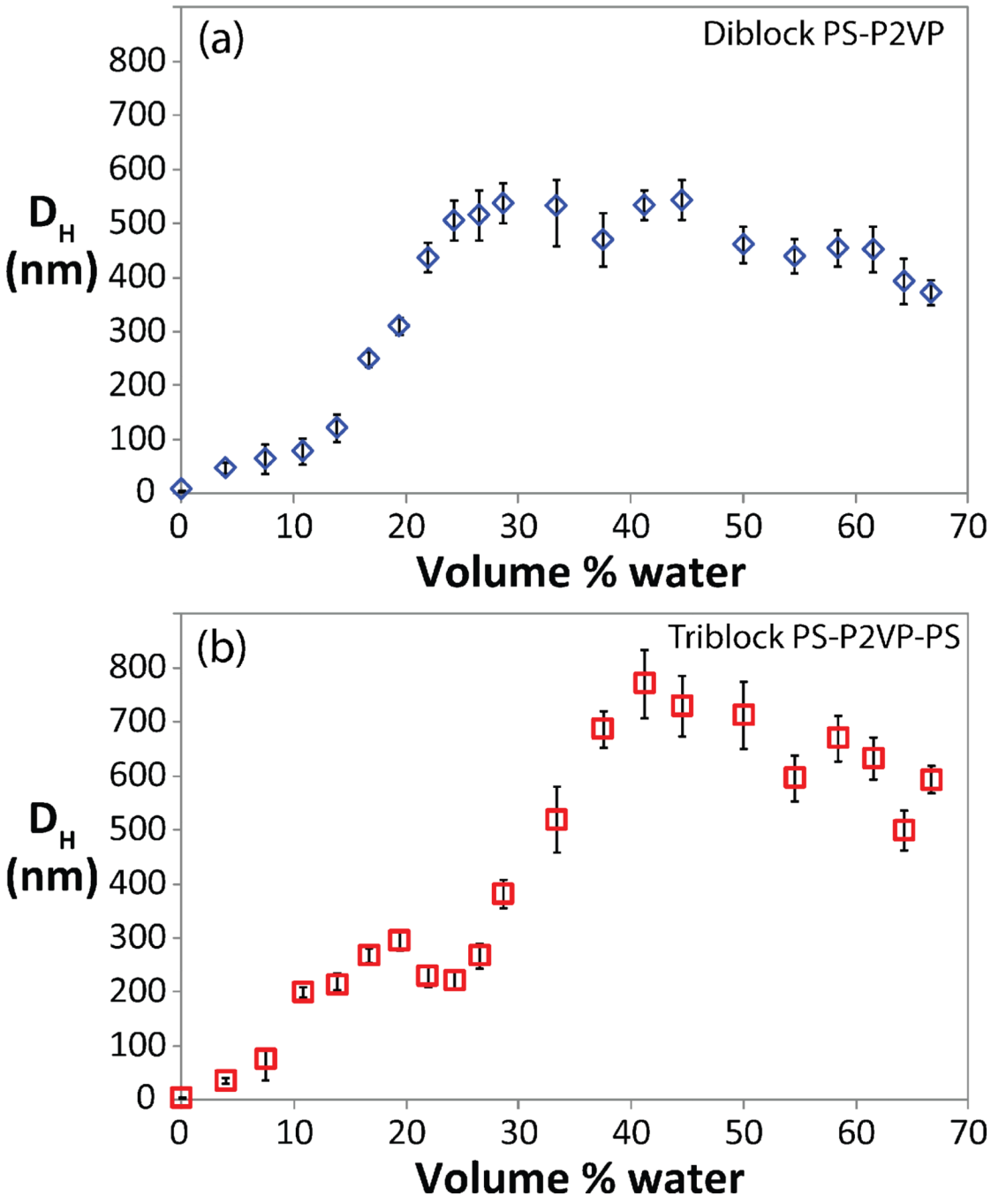

Figure 2.
DLS data demonstrating the growth of particles with respect to water concentration a) diblock copolymer, b) triblock copolymer. Error bars represent one standard deviation as calculated from individual size distributions. Typical size distributions are shown in Figure S2.

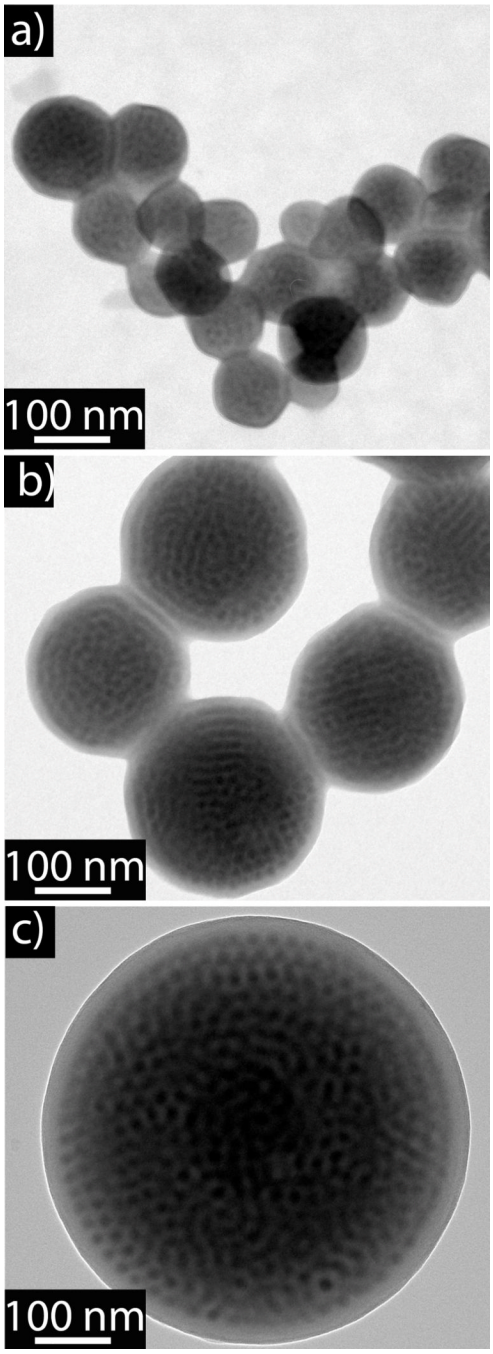

Figure 3.
TEM analysis of controlled particles sizes formed by PS-*b*-P2VP-b-PS triblock copolymers after varying amounts of water addition (a) 7.5 %wt water; (b) 14 %wt water; and (c) 28 %wt water. P2VP phase is stained with iodine.

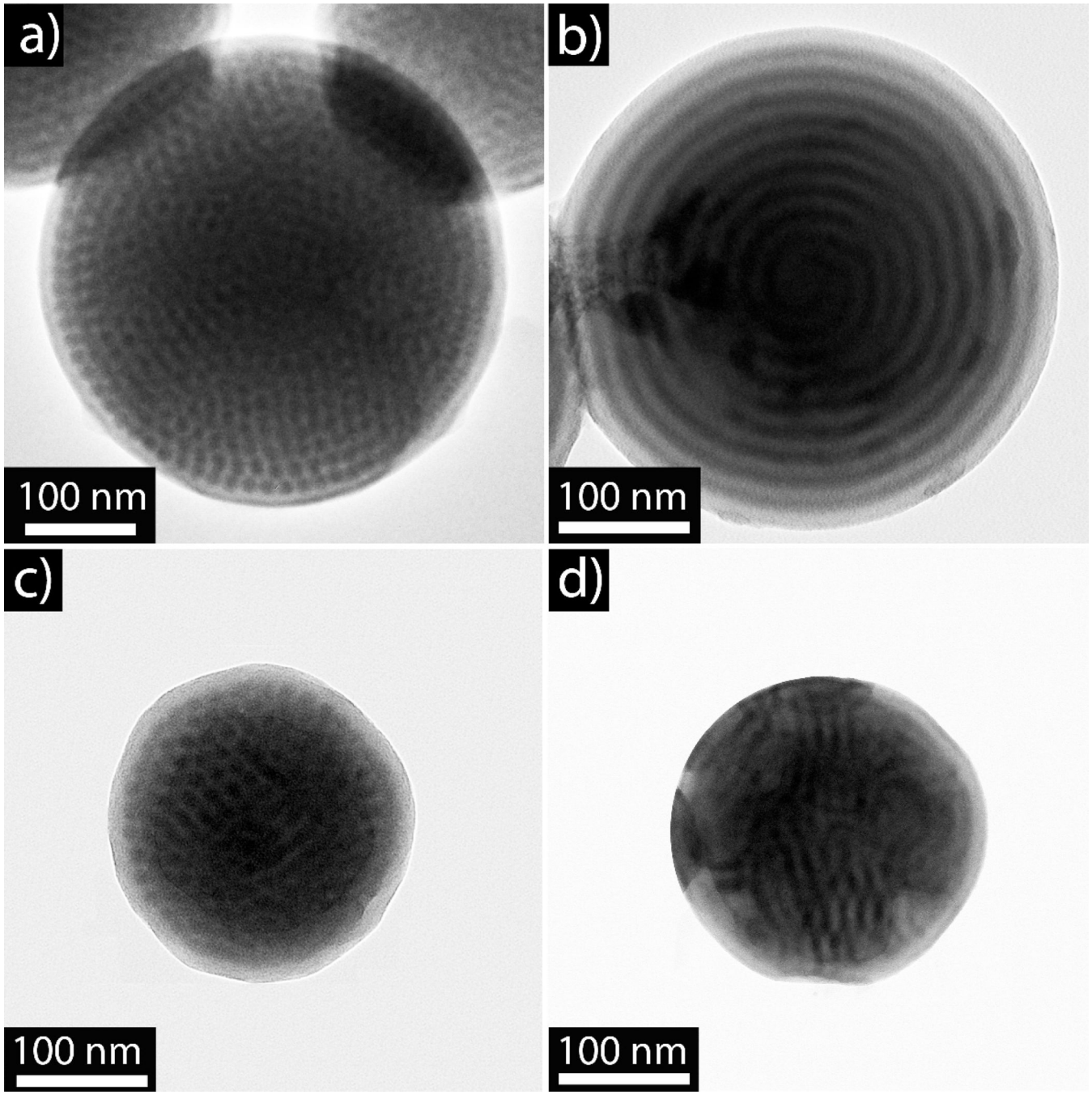

Figure 4.
TEM analysis of phase separated controlled by the particles sizes formed by PS-*b*-P2VP-*b*-PS triblock copolymers a) TEM image of P2VP sphere morphology in PS matrix occurring in a 400nm diameter nanoparticle. b) Onion-like morphology after thermal annealing of the 400 nm particle displayed in a). c) TEM image of triblock copolymer particle (250 nm) formed after the addition of 14 %wt water. d) Disordered lamella-type structure after thermal annealing the 250 nm particles shown in c). P2VP phase is stained with iodine.

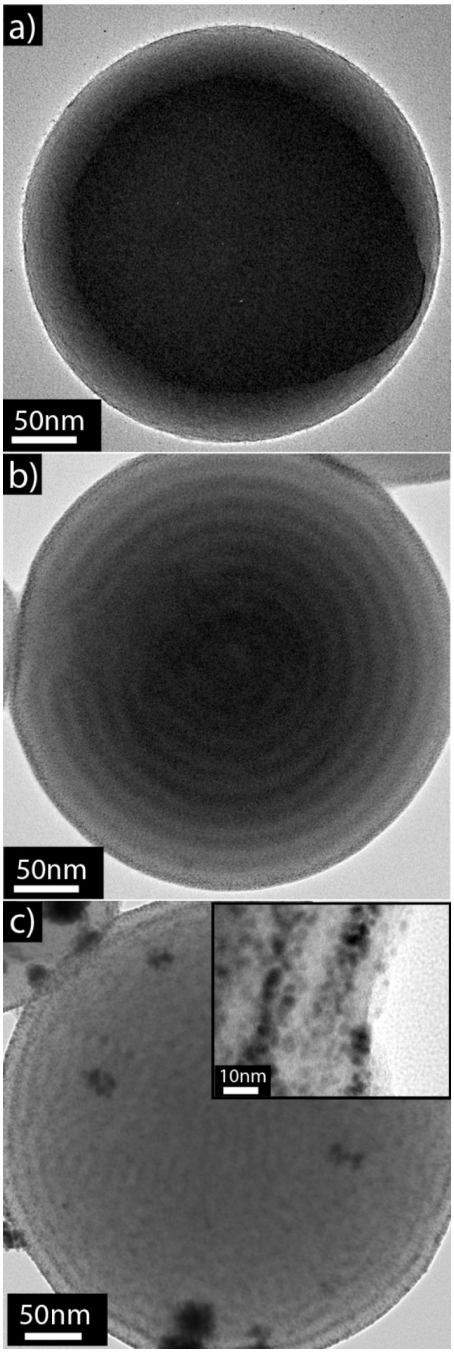

Figure 5.

a) Triblock copolymer nanoparticle without metal salt incubation and no iodine staining showing the absence of contrast in the TEM image. b) $HAuCl_4$ loaded onion-like PS-*b*-P2VP-*b*-PS triblock copolymer particle showing the stained P2VP phase by the gold salt (no iodine staining). c) Gold nanoparticle loaded PS-*b*-P2VP-*b*-PS triblock copolymer particles with onion-like morphology after the absorption and reduction of $HAuCl_4$, insert; high resolution TEM showing sub 10 nm gold nanoparticles.

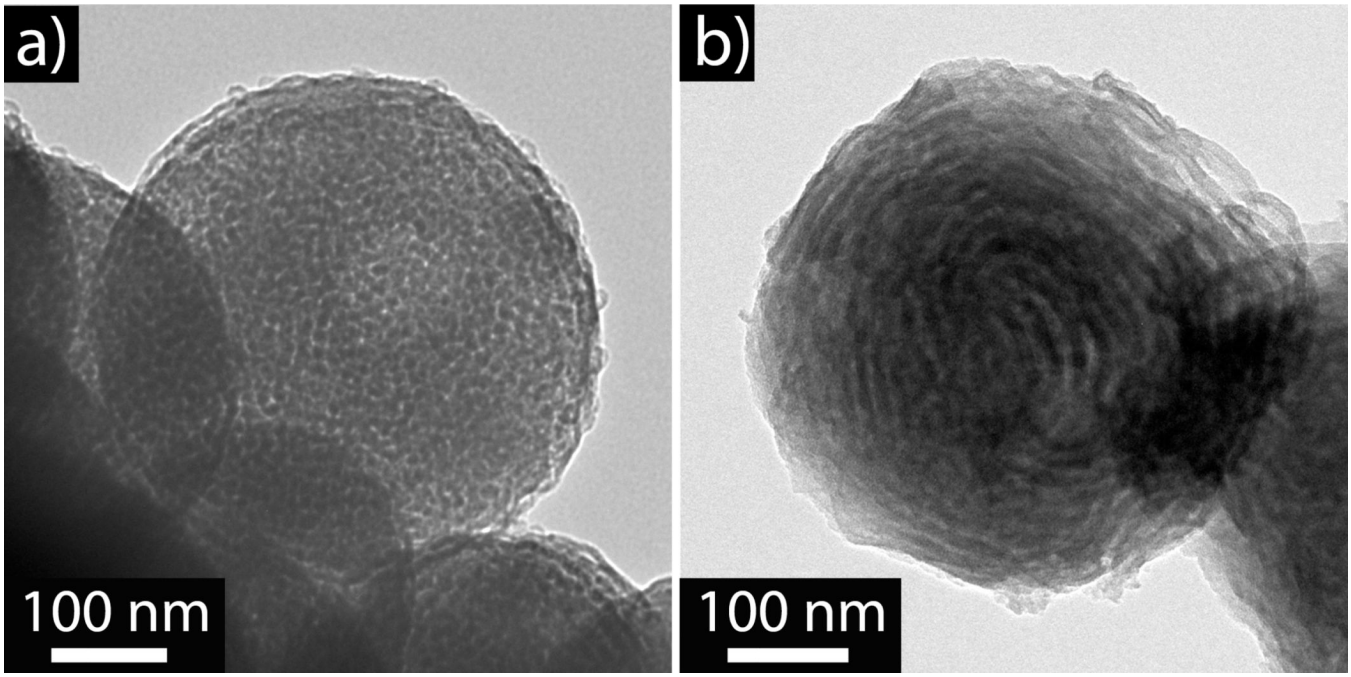

Figure 6.
(a) Silica mesoporous nanoparticle after the removal of the BCP template. (b) Titania onion-like particle after the removal of the BCP template.

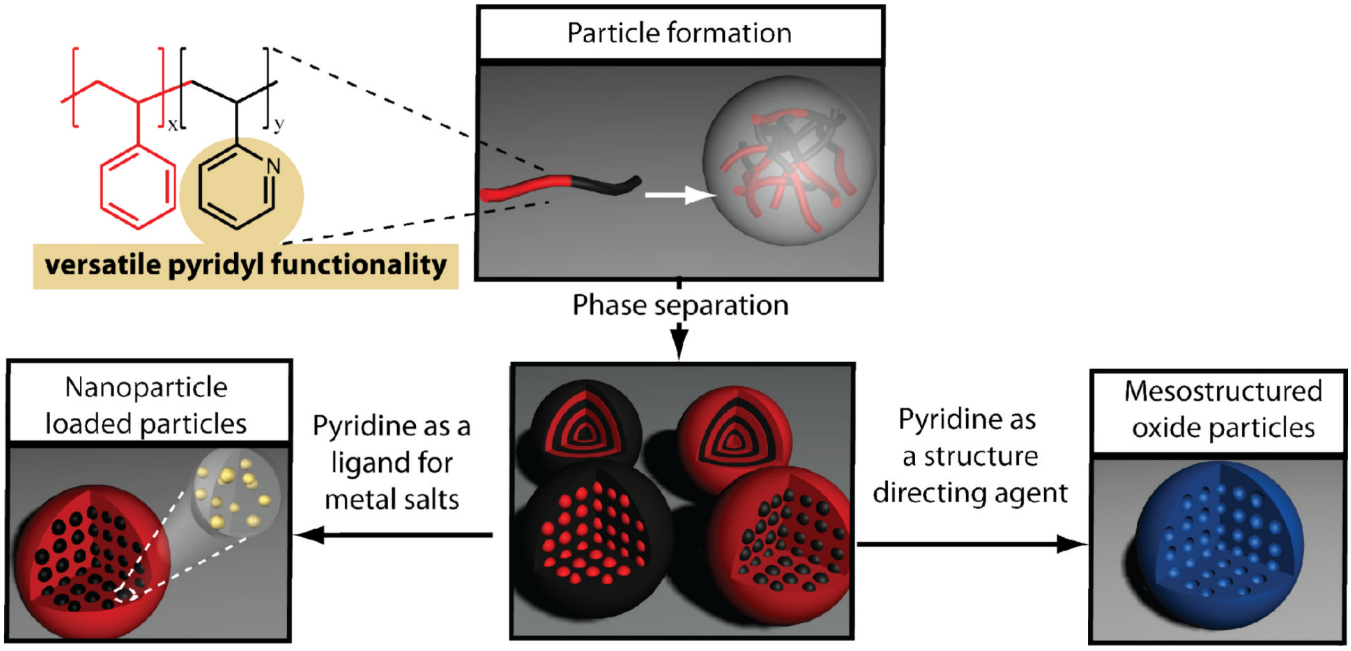

Scheme 1.
Graphical representation of the potential nanostructures and applications for nanoparticles based on block copolymers.